1 Shape Optimization of a Photo Gun

1.1 Geometry

- latest geometry in Figure 1
- corresponding electric field for $p = 3$, $n_{\text{sub}} = 16$, $V_{\text{el}} = -300$ kV and $V_{\text{ar}} = 1$ kV
- (patches $32 \dots 35$ are not entirely correct, missing the correct high voltage adapter)

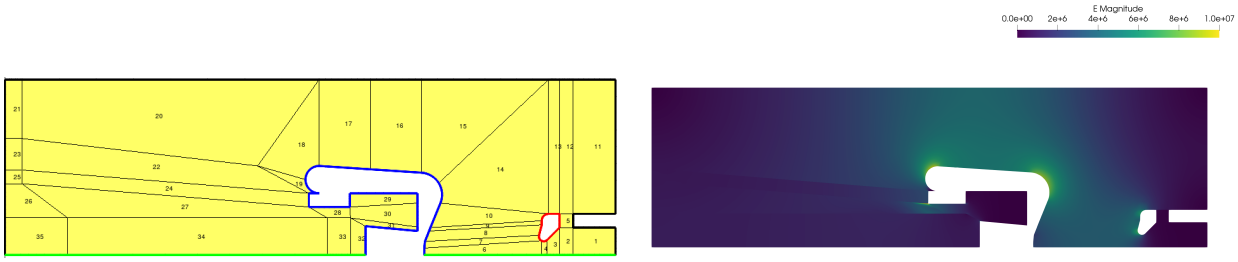

Figure 1: Initial geometry and magnitude of electric field.

1.2 Optimization

- optimized geometry in Figure 2
- cost function only takes into account electric field
- only the upper electrode shape is optimized (volume constraint could be kept as before at 625 cm^3)
- corresponding electric field for $p = 3$, $n_{\text{sub}} = 16$, $V_{\text{el}} = -300$ kV and $V_{\text{ar}} = 1$ kV
- magnitude of E-field remains large in patch 14 (also around anode ring)
- results:

	$(V_{\text{el}} - 625)/\text{cm}^3$	$\max(\|\mathbf{E}\|_2)/\frac{\text{MV}}{\text{m}}$
initial	2.445	9.295
optimized	-12.872	8.49

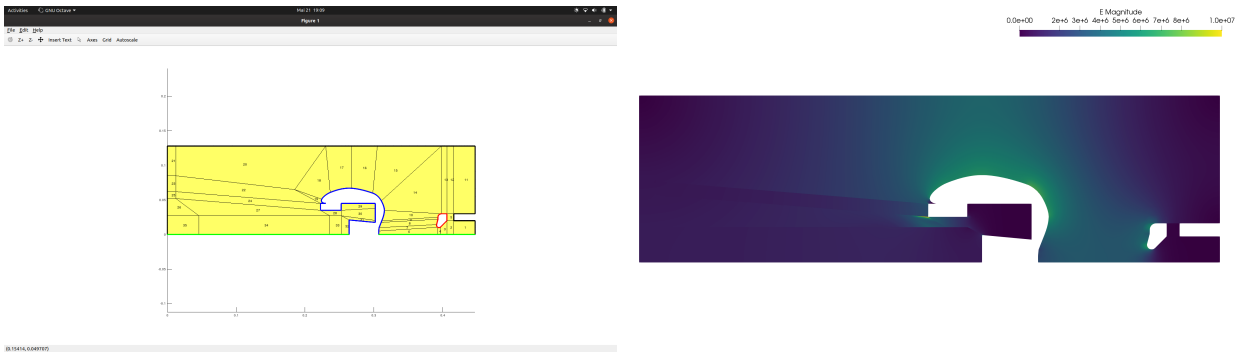

Figure 2: Optimized geometry and electric field.

1.3 Tracking

- general settings: $Q = 100$ fC
- spatial distribution: Gaussian with $\sigma = 400$ μm, see Figure 3 for comparison with laser measurement (probe particles at 0.5σ, σ, 1.5σ in red)
- temporal distribution: Gaussian with $\sigma = 5$ ps, see Figure 4 for comparison with measurement/model from [1]

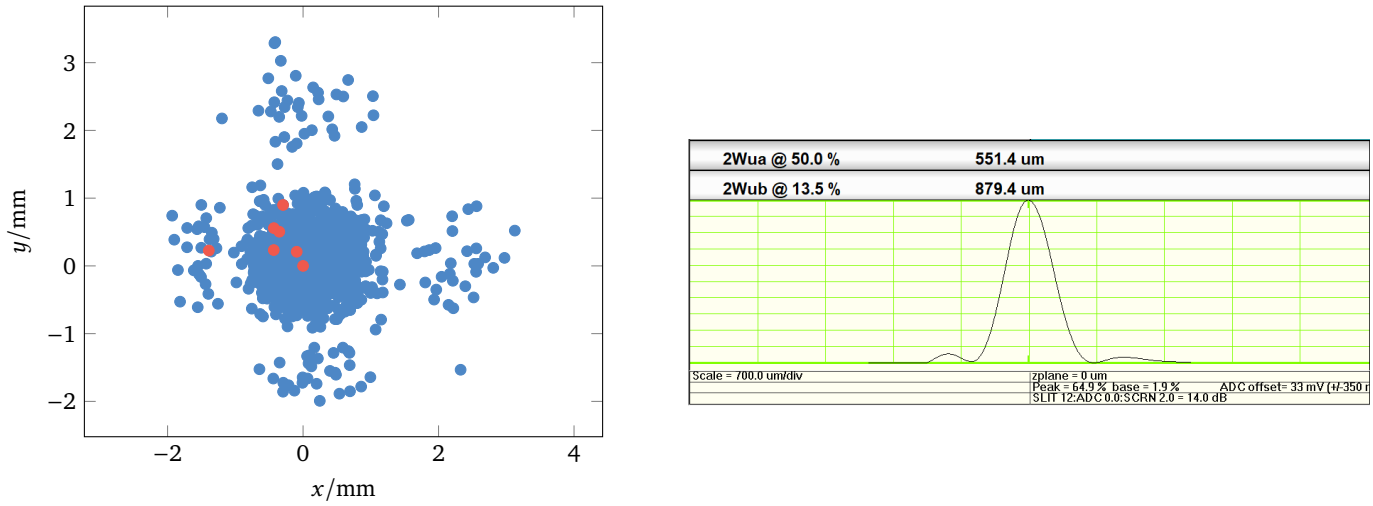

Figure 3: Spatial distribution (2^{10} particles) and laser measurement.

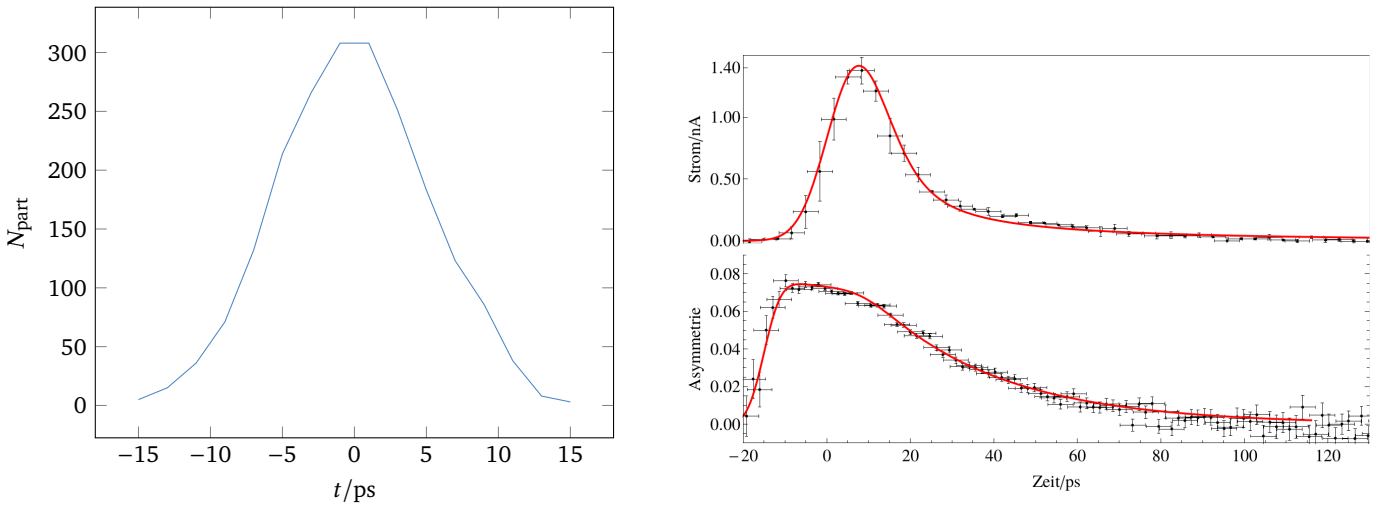

Figure 4: Temporal distribution (2^{10} particles) and measurement/model.

- convergence of time integrator: difference of normalized transverse emmitance ϵ w. r. t. finest time step is shown in Figure 5
- $H = 2^{-11}$ ns used later on

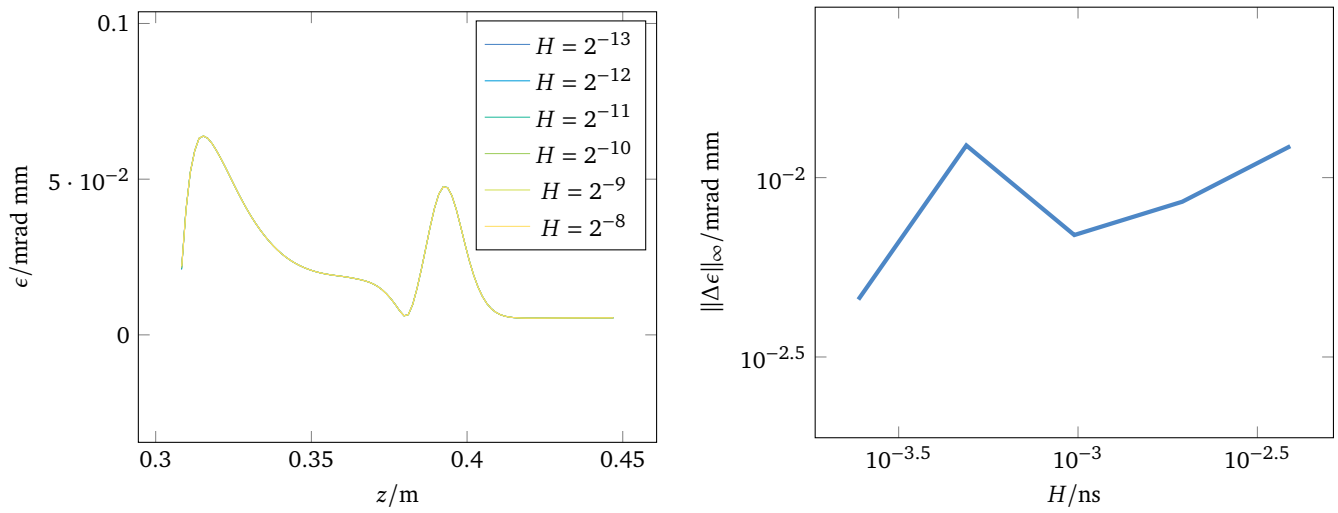

Figure 5: Normalized transverse emmitance and absolute error in l_∞-norm.

- convergence of field map: look at convergence with number of grid points in transverse (n_x, n_y) and longitudinal (n_z) direction individually
- Figure 6 looks at convergence of n_x, n_y for $n_z = 64$
- Figure 7 looks at convergence of n_z for $n_x = n_y = 16$
- $n_x = n_y = 16$ and $n_z = 64$ used later on

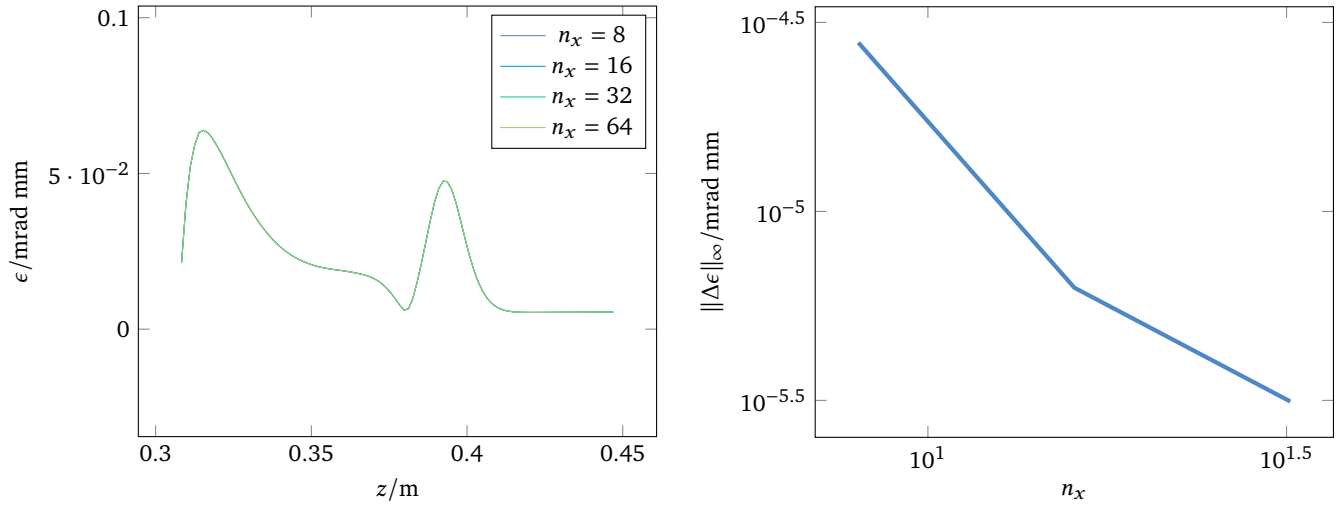

Figure 6: Normalized transverse emmitance and absolute error in l_∞-norm for $n_z = 64$ and $n_x = n_y$ variable.

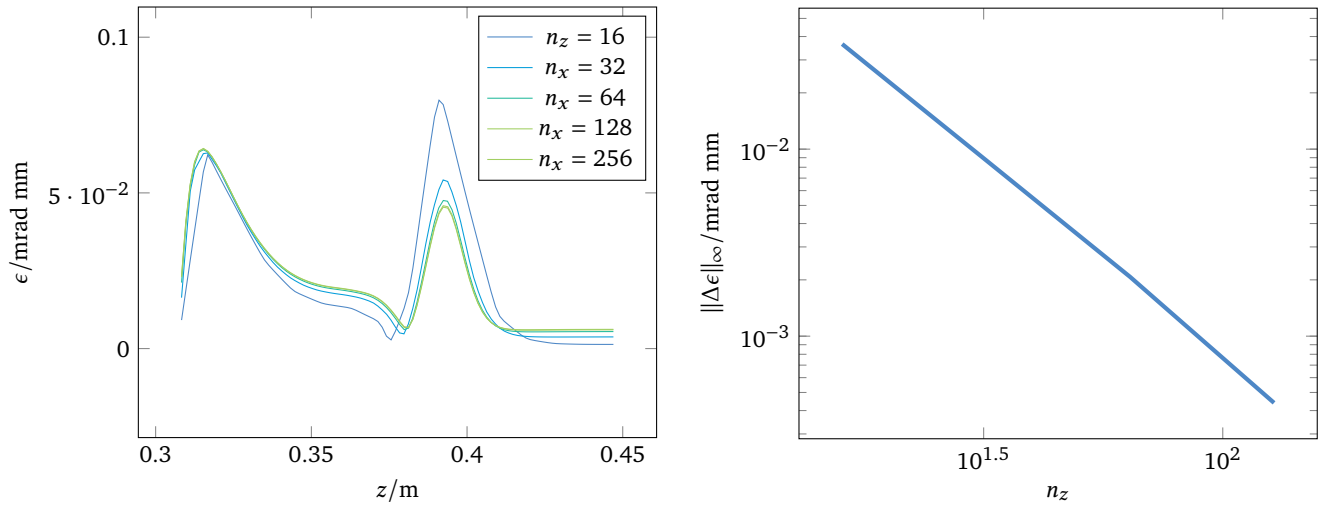

Figure 7: Normalized transverse emmitance and absolute error in l_∞-norm for n_z variable and $n_x = n_y = 16$.

- convergence of space charge: look at convergence with number of grid cells in radial (n_r) and longitudinal (n_l) direction and number of particles (n_I) separately
- Figure 8 looks at convergence of n_r, n_l for $n_I = 2^{10}$
- $n_r = n_l = 16$ used later on
- Figure 10 looks at convergence of n_I for $n_r = n_l = 16$
- $n_I = 2^{10}$

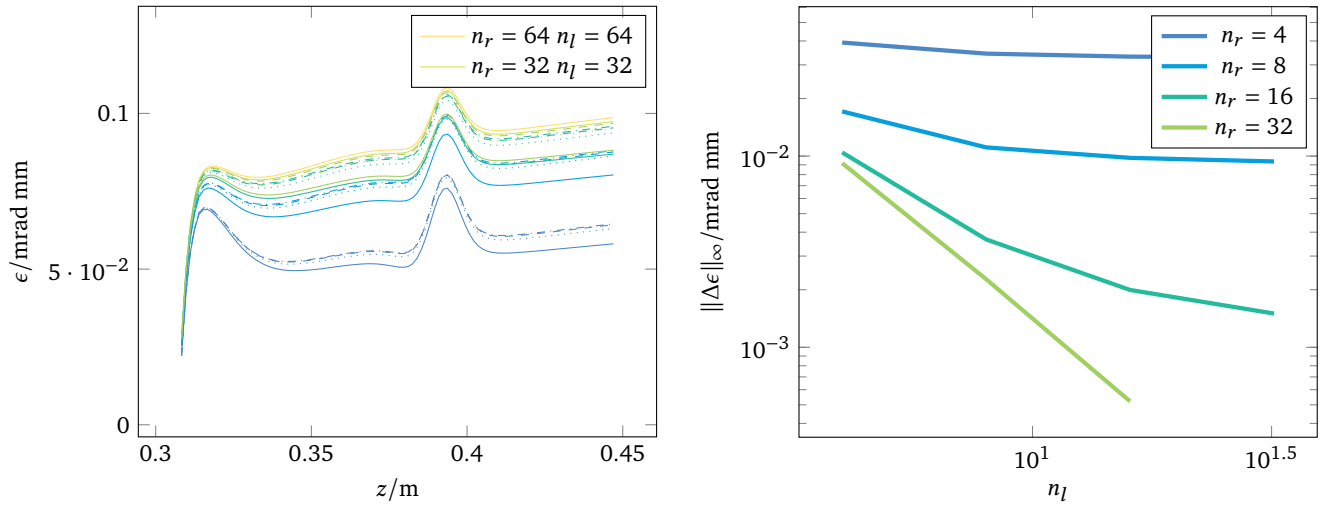

Figure 8: Normalized transverse emmitance and absolute error in l_∞-norm for $n_I = 2^{10}$ and n_l, n_r variable.

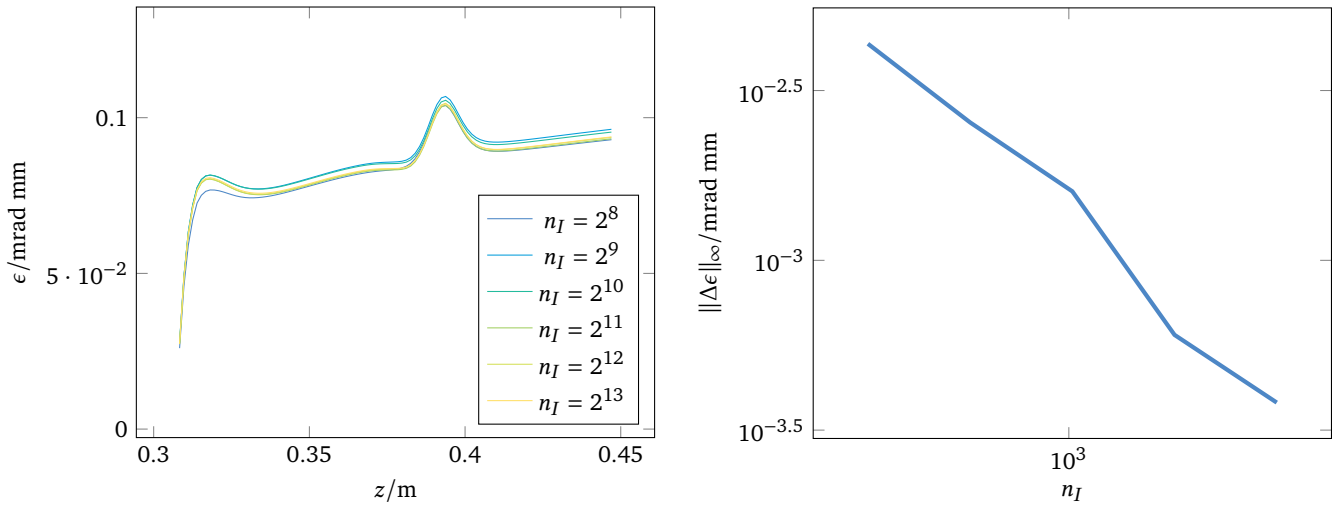

Figure 9: Normalized transverse emmitance and absolute error in l_∞-norm for n_I variable and $n_l = n_r = 16$.

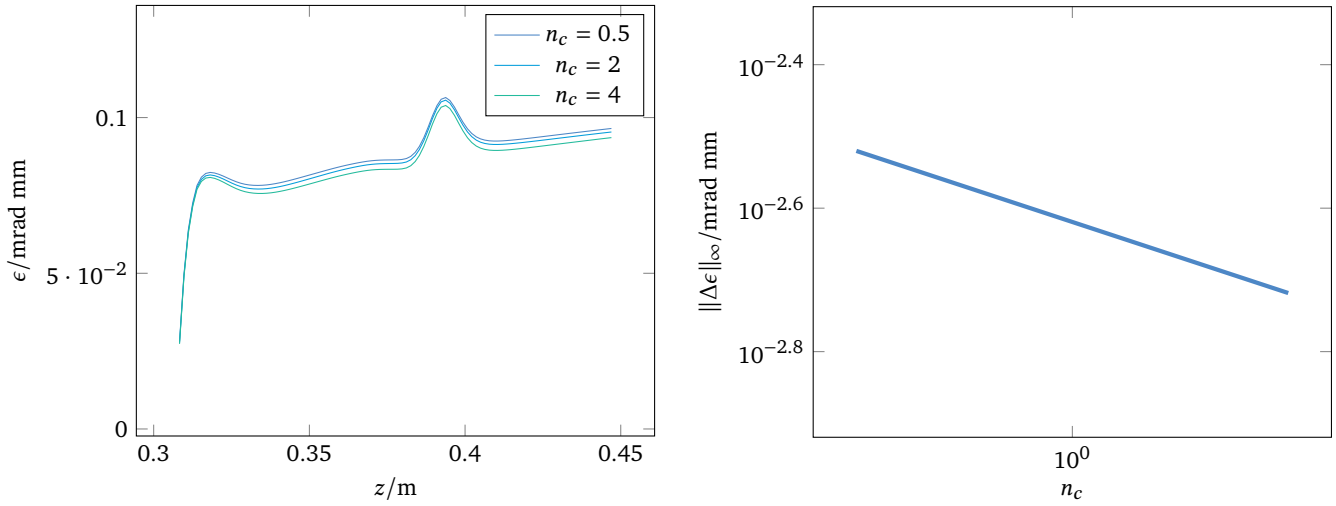

Figure 10: Normalized transversal emmitance and absolute error in l_∞-norm for $n_I = 2^{10}$ and $n_l = n_r = 16$.

- tracking results: ϵ and x_{rms} computed with the determined settings are shown in Figure 11

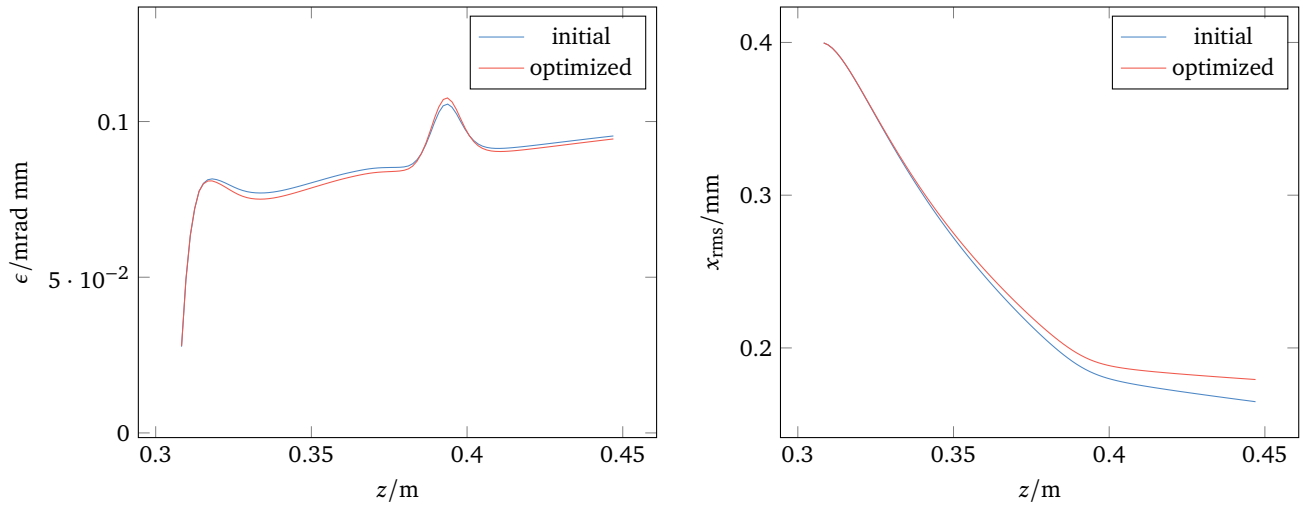

Figure 11: Normalized transverse emmitance and rms beam size.

- remarks: the convergence studies also looked at x_{rms} and the behavior was very similar to that of ϵ
- to minimize the electric field on the entire electrode surface all curves could be taken into account
- this includes the anode ring shape, position and voltage
- also include tracking in optimization via $x_{\mathrm{rms}} \leq 1.5$ mm, also optimize or constrain $\epsilon \leq 1$ mrad mm?

References

[1] Markus Wagner. “Production and investigation of pulsed electron beams at the S-DALINAC”. PhD thesis. Technische Universität Darmstadt, 2013.